

TRANSPORT PROPERTIES IN THE “STRANGE METAL PHASE” OF HIGH T_c CUPRATES: SPIN-CHARGE GAUGE THEORY VERSUS EXPERIMENTS

P. A. Marchetti

Dipartimento di Fisica “G. Galilei”, INFN, I-35131 Padova, Italy

G. Orso

International School for Advanced Studies (SISSA), INFN, Via Beirut, 34014 Trieste, Italy

Z. B. Su and L. Yu

*Institute of Theoretical Physics and Interdisciplinary Center of Theoretical Studies,
Chinese Academy of Sciences, 100080 Beijing, China;*

Center for Advanced Study, Tsinghua University, 100084 Beijing, China

(Dated: February 8, 2020)

The $SU(2) \times U(1)$ Chern-Simons spin-charge gauge approach developed earlier to describe the transport properties of the cuprate superconductors in the “pseudogap” regime, in particular, the metal-insulator crossover of the in-plane resistivity, is generalized to the “strange metal” phase at higher temperature/doping. The short-range antiferromagnetic order and the gauge field fluctuations, which were the key ingredients in the theory for the pseudogap phase, also play an important role in the present case. The main difference between these two phases is caused by the existence of an underlying statistical π -flux lattice for charge carriers in the former case, whereas the background flux is absent in the latter case. The Fermi surface then changes from small “arcs” in the pseudogap to a rather large closed line in the strange metal phase. As a consequence the celebrated linear in T dependence of the in-plane and out-of-plane resistivity is shown explicitly to recover. The doping concentration and temperature dependence of theoretically calculated in-plane and out-of-plane resistivity, spin-relaxation rate and AC conductivity are compared with experimental data, showing good agreement.

PACS numbers: 71.10.Hf, 11.15.-q, 71.27.+a

I. INTRODUCTION: THE “STRANGE METAL PHASE”

In spite of the intensive studies on High T_c superconductors for almost two decades, the phase diagram of this fascinating system is still under debate.¹ One type of phase diagrams is proposed by the RVB scenario,² according to which the temperature-doping concentration plane is divided into four regions: The pseudogap (PG), the strange metal (SM), the superconducting (SC) state and the Fermi liquid (FL) state. An alternative is the quantum critical point (QCP) scenario³ assuming the existence of a QCP under the SC dome controlling the behavior of the system in a rather large quantum critical regime. In a sense that regime corresponds to the SM phase in the RVB picture, the difference being that the PG phase in the QCP scenario has a true long range order, and the boundary between PG and SM phases is a phase transition line, whereas in the RVB picture it is a crossover and it coincides with the superconducting transition line at high dopings. There are several theoretical as well as “experimental” proposals on the origin of the QCP.^{4,5,6,7,8,9,10}

Recently, we have developed a spin-charge gauge approach to describe the PG phase in cuprate superconductors, particularly focusing on the metal-insulator crossover (MIC) phenomena.^{11,12,13,14,15} Within a unified framework we have calculated the in-plane and out-of-plane resistivity, including the effect of external magnetic field, optical conductivity, nuclear magnetic resonance (NMR) relaxation rate and the spectral weight of the electron Green’s function, in good agreement with experimental data. In this approach based on spin-charge decomposition applied to the 2D t - J model, the spinon dynamics is described by a nonlinear σ -model with a theoretically derived mass gap $m_s \sim J(\delta |\ln \delta|)^{1/2}$, where J is the exchange integral, δ the doping concentration; the holon is fermionic with “small” Fermi surface (FS) ($\epsilon_F \sim t\delta$) (with t as the hopping integral) centered around $(\pm\pi/2, \pm\pi/2)$ in the Brillouin zone and a “Fermi-arc” behavior for the spectral weight. Both holons and spinons are strongly scattered by gauge fluctuations. As an effect of gauge interactions, the spinon mass picks up a dissipative term: $m_s \rightarrow M_T = (m_s^2 - icT/\chi)^{1/2}$, where $\chi \sim t\delta^{-1}$ is the diamagnetic susceptibility and c a numerical constant. This shift in turn introduces a dissipation in the spinon-gauge sector, whose behavior dominates the low energy physics of the system. The competition between the mass gap and the dissipation is responsible for the MIC, giving rise to a broad peak in the DC conductivity. At low temperatures the antiferromagnetic (AF) correlation length $\xi \sim m_s^{-1}$ is the determining scale of the problem, leading to localizing behavior, while at higher temperatures, the de Broglie wave length $\lambda_T \sim (\chi/T)^{1/2}$ becomes comparable, or even shorter than ξ , giving rise to metallic conductivity.

Since this theory was originally^{11,14} formulated to describe the MIC in the in-plane resistivity ρ_{ab} and related phenomena taking place in the PG “phase”, its range of applicability was therefore limited to underdoped systems and low temperatures where the AF correlation length ξ is smaller or of the order of the thermal de Broglie wavelength λ_T . In fact, our theory correctly describes the low-temperature insulating behavior and MIC up to the inflection point T^* where the second derivative of ρ *w.r.t.* temperature vanishes. However, the “high temperature asymptotics” derived from the theory $\rho \sim T^{1/4}$ is not correct. At higher temperatures $T \sim T^*$, the PG temperature, underdoped cuprates crossover to a new, SM “phase”. Overdoped cuprates also reach this phase increasing T , but presumably from an ordinary FL state. The SM phase is *metallic* in nature with anomalous yet rather simple temperature dependence of physical observables such as the celebrated T –linearity of both in-plane and out-of-plane resistivity at sufficiently high temperatures.

Experimentally, the SM phase shares with the PG phase an AF short range order (SRO) which in our approach originates from the gapping of spin waves due to scattering against spin vortices attached to the moving holes. There are strong indications, in particular from the angle-resolved photoemission spectroscopy (ARPES) experiments,¹⁶ that charge degrees of freedom undergo instead a radical rearrangement near the crossover temperature T^* : the excitations far from the zone diagonals, *i.e.*, located near $(\pi, 0)$ of the Brillouin zone, become gapless and lead to a *large* closed FS. This means that the density of *effective* charge carriers has grown from δ , characteristic of the PG phase, to $1 - \delta$, the value expected from the band structure calculations.

The transport and optical properties in the SM phase were considered earlier by various theoretical treatments, including the slave-particle mean field theory,¹⁷ the gauge field approach,^{18,19,20} “nearly AF Fermi liquid” theory,²¹ and the closely related spin-fermion model.⁹ In the last approach a special role is assigned to the “hot spots”, *i.e.*, those points on the FS, separated by the AF vector (π, π) from their counterparts. As a kind of opposite limit, the “cold spots” (intersections of FS with zone diagonals) model was also considered,²² where these “cold spots” are argued to dominate the in-plane and out-of-plane transport properties. However, it is fair to say that a complete understanding of the diversified experimental findings in this unusual phase is still lacking.

In this paper we generalize our spin-charge gauge approach to consider the SM phase, and compare the calculated transport properties with experimental data in this regime. The AFSRO and the gauge field fluctuations which were the key ingredients in the theory for the PG phase still play an important role here. The main difference, however, is the following: In the PG phase near half filling there is an underlying statistical π -flux lattice for holons. As the doping (or temperature) increases, this π -flux lattice is more and more disturbed, and at certain point it “melts”. The energetically favorable configuration should now correspond to zero flux, instead of π -flux (*Assumption 0*). It turns out that our spin-charge gauge approach can be generalized to this case to describe the large FS instead of “Fermi-arcs”. As a consequence the celebrated linear in T dependence of in-plane and out-of-plane resistivity is shown explicitly to recover. Since the formalism is similar, we will only sketch the major steps, referring the reader to our previous papers Refs. 11,14 for more detail. The rest of the paper is organized as follows: the spin-charge gauge approach is outlined in Sec. II, while the effects of the gauge field are considered in Sec. III. The comparison of theoretical results with experimental data on in-plane and out-of plane resistivity, NMR relaxation rate and AC conductivity is presented in Sec. IV with some brief concluding remarks in Sec. V. The proof that one can satisfy the *Assumption 0* for the free energy minimum is given in the Appendix.

Readers only interested in the final theoretical results for the SM phase and comparison with experiment can skip Secs. II and III, and go directly to Sec. IV.

II. SPIN-CHARGE GAUGE APPROACH

As mentioned above, to discuss the “SM phase” we follow the same strategy as that adopted for the “PG phase”. Therefore we outline the changes instead of repeating the whole procedure. The discussion however will be sufficiently complete that using Refs. 11,14 as a guide the interested reader will have no difficulty to fill in the missing details. From now on we adopt the system of units: $J = a = 1$, where a is the lattice constant.

We assume as a model for CuO layers in high T_c cuprates the 2D t - J model and we treat it in an “improved Mean Field Approximation”(MFA) via a gauge theory of spin-charge decomposition, obtained by gauging the global spin and charge symmetries of the model introducing Chern-Simons (C-S) gauge fields. To the fermion c of the gauged model we apply the spin-charge decomposition: $c \sim H z_\alpha$, where H is the holon, a charged spinless fermion, and z_α is the spinon, neutral spin 1/2 boson of a nonlinear σ model. To derive the MFA a key step is to find a “reference spinon configuration” *w.r.t.* which one expands the fluctuations described by z_α . Such reference configuration was found by optimizing the free energy of holons in a self-consistently fixed holon-dependent spinon background, in a kind of Born-Oppenheimer approximation. In Ref. 14 it has been shown that a lower bound on this free energy can be obtained via the optimization of the free energy of a gas of spinless holes with the same density of holons, on a square lattice, with n.n. hopping parameter given by $tU_{<ij>}$. Here $U_{<ij>}$ is a time-independent complex gauge field

related to the C-S charge and spin gauge fields, denoted by B and V , respectively, by

$$U_{\langle ij \rangle} \sim e^{-i \int_{\langle ij \rangle} B} (\sigma_x^{|i|} (P e^{i \int_{\langle ij \rangle} V}) \sigma_x^{|j|})_{11}, \quad (1)$$

where P denotes the path-ordering, σ_x the Pauli matrix and $|i| = 0$ if i is a site on the Néel sublattice containing the origin and $|i| = 1$ if i is on the other Néel sublattice.

At low temperature and small doping concentration, *i.e.* in the parameter region to be compared with the “PG phase” of the cuprates, it has been argued in Ref. 11 that the optimal configuration of U carries a flux π per plaquette and it has been shown that one can find configurations of B and V reproducing this behavior on average. Then neglecting the feedback of holon fluctuations on B and that of spinon fluctuations on V , the charge C-S gauge field B carries flux π per plaquette and via Hofstadter mechanism converts the spinless holon H into a Dirac fermion with a small FS centered at the four nodes $(\pm \frac{\pi}{2}, \pm \frac{\pi}{2})$; the spin C-S gauge field V dresses the holons with spin vortices and the spinons in this gas of “slowly moving dressed holons” acquire a mass $m_s \sim J \sqrt{|\delta \ln \delta|}$ consistent with AF correlation length at low dopings derived from the neutron experiments.²⁴

Dirac holons and massive spinons are coupled by a $U(1)$ slave-particle gauge field A , called h/s in Ref. 11. The low energy effective action for A is obtained upon integration of the matter fields and since holons have a non-vanishing density at the FS, it exhibits a Reizer singularity²⁵ dominating at large scales: for small $q, \omega, \omega/|q|$

$$\langle A^T A^T \rangle(\omega, \vec{q}) \sim (\chi |\vec{q}|^2 + i\kappa\omega/|\vec{q}|)^{-1}, \quad (2)$$

where $\chi \sim \delta^{-1}$ is the diamagnetic susceptibility and $\kappa \sim \delta$ the Landau damping. In turn the Reizer singularity produces as the leading effect¹² a shift in the mass of spinons $m_s \rightarrow M = (m_s^2 - icT/\chi)^{1/2}$, where $c \sim O(1)$ is a positive constant, thus producing a dissipation, linear in T at low temperatures. The competition between the two energy scales m_s^2 and T/χ , related to the spinon gap and dissipation is the root in the spin-charge gauge approach of many crossover phenomena peculiar to the transport properties of the “PG phase”.

In our approach, the increase in the density of state at the Fermi energy ε_F as we move from the PG to the SM “phase” reflects a change in the holon dispersion relation. The π -flux statistical field that minimizes the ground state energy near half filling was responsible for the small FS in the PG phase. Since the SM is metallic in nature, we expect that in this phase there are no statistical magnetic fields to frustrate the charge motion and therefore we make the following

Assumption 0: In the optimal configuration (for the range of parameters corresponding to the SM phase) the flux per plaquette carried by U is 0, *i.e.*

$$\arg(U_{\partial p}) = 0. \quad (3)$$

In favor of this assumption we can offer the following argument: It has been rigorously proved by Lieb²⁶ that at half filling the optimal configuration for a magnetic field on a square lattice is translationally invariant, with flux π for each plaquette at arbitrary high temperature. On the other hand, it is well known that at low density and high temperature the optimal configuration has zero flux per plaquette. At zero temperature it has been proved that the ground state energy has a minimum corresponding to one flux quantum per spinless fermion.²⁷ Numerical simulations suggest that increasing the temperature gives rise to a competition between these minima and at high temperatures only the zero flux and π -flux configurations survive.²⁸ Therefore one can argue that at sufficiently high doping and temperature *Assumption 0* is satisfied. By analyticity it is then reasonable to assume it holds in the entire SM phase except near the crossover boundaries to other “phases”. Taking *Assumption 0* for granted, we show explicitly in the Appendix that (under the same approximation as used for the PG phase) one can find a gauge field configuration that satisfies it on average, so that our spinon field z_α will describe the fluctuations around it. The outcome of this optimization is that in the SM phase the flux carried by the charge gauge field responsible for the statistical flux in the PG phase is cancelled by the flux carried by the spin gauge field on average.

The flux change does not affect the spinon action, therefore it is formally identical to that considered for the PG case, thus leading to the same low energy effective action

$$S = \int d^3x \frac{1}{g} \left[v_s^{-2} |(\partial_0 - iA_0) z_\alpha|^2 + |(\partial_\mu - iA_\mu) z_\alpha|^2 + m_s^2 z_\alpha^* z_\alpha \right], \quad (4)$$

where $g \sim J^{-1}$, $v_s \sim J$, $x = (v_s x^0, \vec{x})$, $A = (v_s A_0, \vec{A})$. This implies that in our approach the AFSRO is characteristic of both PG and SM phases; however we will see that in the SM phase it is less effective. The action derived above is for $T = 0$ and it can be argued to be correct only for temperature smaller than the mass gap; one can improve the situation by approximately taking into account finite temperature correction by including in the action the spinon thermal mass

term found in the classical renormalized region of the model,²⁹ with thermal mass $m_T \sim (2\pi\rho_s/J)e^{-2\pi\rho_s/T}$, where ρ_s is the renormalized spin stiffness. If we adopt for $2\pi\rho_s$ the value (150 meV) used in fitting the inverse magnetic correlation length of underdoped samples of LSCO in Ref. 29, the order of magnitude and the qualitative temperature and doping dependence of the experimental data are reproduced using the above derived formula $m_s(T) = (m_s^2 + m_T^2)^{1/2}$. The renormalized classical formula holds only for $T \ll 2\pi\rho_s$ and it has been argued to be correct up to roughly 500 K and this yields an upper limit of validity of the above treatment.

We now turn to holons. The change of statistical flux does affect deeply the holon motion. Since we would like to find eventually the continuum low-energy action, we expand the holon action in powers of the lattice constant keeping the leading order, and the result rewritten in the lattice form is:³⁰

$$S_h(H, H^*, A) = \int d^3x \left[\sum_j H_j^* (i\partial_0 - \mu - A_0) H_j + \sum_{\langle ij \rangle} (t H_i^* H_j e^{i \int_{\langle ij \rangle} A} + h.c.) \right], \quad (5)$$

where μ is the chemical potential, A_μ denotes the slave-particle self-generated h/s gauge field as in the PG phase. Neglecting gauge fluctuations, the dispersion relation for holons has changed from the π -flux phase spectrum

$$\epsilon^{PG}(\vec{p}) = \pm 2t \sqrt{\cos^2(p_x) + \cos^2(p_y)}$$

restricted to the magnetic Brillouin zone to the more conventional tight binding spectrum

$$\epsilon^{SM}(\vec{p}) = 2t(\cos(p_x) + \cos(p_y))$$

defined in the entire Brillouin zone.

Then the FS is obtained by filling all the states up to $\mu \sim 4t\delta$ resulting in a large closed FS, contained in the reduced Brillouin zone and the bottom of the band for the holon is at the corners of the Brillouin zone. To write a continuum limit for the holon action, first as a crude approximation we substitute the FS with a circle having the same volume and then make a *particle/hole* conjugation $H_i \rightarrow E_i^*$. Due to this approximation (and neglecting from beginning the n.n.n. hopping) all features depending on the detailed structure of the FS are clearly lost. The tight binding action defined on the square lattice is then replaced by a continuum action describing free particles ($\epsilon_k = k^2/2m^*$) with an effective chemical potential $\epsilon_F \sim 4t(1 - \delta)$, where $-4t$ corresponds to the bottom of the tight binding band, assuming that the field E has a well-defined continuum limit. By “abuse” of language, we still call E holon field. The continuum low energy action for E is given by:

$$S(E) = \int d^3x \left[E^*(x^0, \vec{x}) (i\partial_0 - \epsilon_F - A_0 - \frac{1}{2m^*} (\vec{\nabla} - i\vec{A})^2) E(x^0, \vec{x}) \right]. \quad (6)$$

Since spinons are massive and the charge carriers (holons in the above sense) described by E are gapless with a finite FS, the low-energy effective action for A exhibit a Reizer behaviour as in the PG phase. Using the above simplified action, the Landau damping and diamagnetic susceptibility can be easily evaluated and have a weak dependence on the doping concentration in the relevant range $\delta \lesssim 0.3$. First note that $v_F \sim 2t$ is doping independent, $k_F \propto (1 - \delta)$ and therefore $m^* = k_F/v_F = (1 - \delta)/2t$. The parameters entering the Reizer propagator (2) are then given by

$$\kappa \sim O(1 - \delta), \quad (7)$$

$$\chi \sim 1/12\pi m^* \sim \frac{t}{6\pi(1 - \delta)}, \quad (8)$$

assuming that the holons give the dominating contribution (certainly true for sufficiently high δ) to χ .

The main difference *w.r.t.* the PG estimates¹⁴ is that δ is now replaced by $(1 - \delta)$ so that, roughly speaking, both quantities vary by a factor of the order 5 – 10.

The decrease of the diamagnetic susceptibility implies that the thermal de Broglie wavelength for holons is shorter *w.r.t.* the PG analogue and therefore the spin-gap effects ($\xi^2 < \lambda_T^2$) are less effective, being confined to very low temperatures. As a result, gauge fluctuations in the spinon sector strengthen and dominate over the spin gap at all temperatures down to T^* for the underdoped samples, thus determining the thermal behavior of many physical properties. In particular we shall recover some of the distinctive features of the SM, namely the T -linearity of in-plane, out-of-plane resistivities and spin lattice relaxation time (T_1T)⁶³ up to several hundreds Kelvin.

The low energy effective action obtained in our approach bears some resemblance with the one derived in the slave boson approach,¹⁸ with however two basic differences: the statistics of holon and spinon is interchanged and the bosons in our spin-charge gauge approach are massive, due to the coupling to spin vortices absent in the slave boson approach, and “relativistic” due to AFSRO; in the slave boson approach, instead, they are non-relativistic and gapless. In a sense our effective action is closer to the slave fermion ansatz outlined in Ref. 19, although the starting point is quite different.

III. GAUGE FIELD EFFECTS

In this Section we summarize the physical consequences of the gauge field fluctuations, expressed in terms of spin and electron Green’s functions.

The h/s gauge field A renormalizes the massive spinons in a nontrivial way. The expression obtained for the *dressed* magnon (or spin-wave) correlator by summing up the gauge fluctuations via an eikonal approximation obtained for the PG phase applies here as well:

$$\langle \vec{\Omega}(x) \cdot \vec{\Omega}(0) \rangle \sim \frac{1}{(x^0)^2 - |\vec{x}|^2} e^{-2i\sqrt{m_s^2 - \frac{T}{\chi} f(\frac{|\vec{x}|Q_0}{2})} \sqrt{(x^0)^2 - \vec{x}^2} - \frac{T}{2\chi} Q_0^2 g(\frac{|\vec{x}|Q_0}{2}) \frac{(x^0)^2 - |\vec{x}|^2}{m_s^2 - \frac{T}{\chi} f(\frac{|\vec{x}|Q_0}{2})}}. \quad (9)$$

provided the new estimates for κ and χ are used. The functions f and g contain the information on major effects due to the interaction with the gauge field and their explicit expression can be found in Ref. 14. $Q_0 = (\kappa T/\chi)^{1/3}$ is a momentum cutoff and Q_0^{-1} can be identified as the length scale of gauge fluctuations, analogous to the anomalous skin depth. It is important to note that, *w.r.t.* the PG estimate, the new momentum scale $Q_0 \approx \frac{(1-\delta)^{(2/3)}}{a} \left(\frac{6\pi T}{t}\right)^{1/3}$ is almost doping independent and is roughly $(\delta)^{-2/3}$ bigger. If one integrates over $|\vec{x}|$ in the range $T^{-1} \gg x^0 \gg |\vec{x}|$ and makes use of the definition of Q_0 for the SM phase, the contribution of the complex saddle point that dominated the integral in the PG phase turns out to be small compared with the contribution coming from fluctuations around the coordinate origin, in the region $|\vec{x}|Q_0 \lesssim 1$, for T or δ sufficiently large. Expanding f and g to leading order around the origin one derives:

$$\langle \vec{\Omega}(x) \cdot \vec{\Omega}(0) \rangle \simeq \frac{1}{x^0{}^2} e^{-2im_s x^0 + i\frac{T}{\chi m_s} \frac{|\vec{x}|^2 Q_0^2}{24} x^0} e^{-\frac{T}{2\chi} Q_0^2 g(0) \frac{x^0{}^2}{m_s^2}}. \quad (10)$$

The integration over $|\vec{x}|$ is then simply Gaussian; defining

$$a = \frac{T}{\chi m_s} \frac{Q_0^2}{24} x^0 \quad (11)$$

and assuming $|a| \gg Q_0^2$, we are allowed to remove the cut-off (the small real convergence factor needed can be supplied by the neglected higher order terms) obtaining (in the Fourier transformed representation for the space coordinates):

$$\langle \vec{\Omega} \cdot \vec{\Omega} \rangle(x^0, \vec{q}=0) \simeq \frac{1}{x^0{}^2} e^{-2im_s x^0 - \frac{T}{2\chi m_s^2} g(0) Q_0^2 x^0{}^2} \int_{|\vec{x}|Q_0 \lesssim 1} e^{ia|\vec{x}|^2} |\vec{x}| d|\vec{x}| \simeq \frac{ie^{-2im_s x^0 - \frac{T}{2\chi m_s^2} g(0) Q_0^2 x^0{}^2}}{ax^0{}^2}. \quad (12)$$

The real part of the exponent in (12) is monotonically decreasing in x^0 , therefore we estimate the x^0 integral by principal part evaluation. Since our approach is valid only at large scales, we introduce an UV cutoff in the integral at λQ_0^{-1} and evaluate the integration assuming λ large. Then we make the tentative conjecture that for small ω the physics is dominated by large scales and the small-scale contribution can be taken into account phenomenologically by a suitably chosen rescaling of λ (it cannot be sent to 0 as in the PG phase, because here for $\lambda=0$ the exponent loses its convergence factor). The result of this approximation is:

$$\langle \vec{\Omega} \cdot \vec{\Omega} \rangle(\omega, \vec{q}=0)|_{\omega \rightarrow 0} \simeq \frac{\chi m_s Q_0}{T} \frac{e^{i(\omega - 2m_s)\lambda Q_0^{-1} - \frac{T}{2\chi m_s^2} g(0)\lambda^2}}{\omega - 2m_s + i\frac{T}{\chi m_s^2} g(0)Q_0\lambda}. \quad (13)$$

This result appears physically reasonable if the exponent in (13) is slowly varying and of the order 1; this puts limits, *a priori* on the validity of the above conjecture given by:

$$\begin{aligned} T &\gtrsim (2m_s\lambda)^3 \chi/\kappa \sim \lambda^3 t(\delta|\ln\delta|)^{3/2}, \\ T &\lesssim 2\chi m_s^2/(g(0)\lambda^2) \sim \lambda^{-2} t\delta|\ln\delta|. \end{aligned} \quad (14)$$

A posteriori, self-consistently $\lambda \sim O(1)$ (from fitting $\lambda \approx 0.7$), and (14) selects a range roughly between few tens and few hundreds Kelvin ($\approx 2 - 5$ for $\delta \approx 0.04 - 0.15$; for higher dopings the upper limit of the temperature-dependent mass treatment²⁹ $\approx 500K$ applies). In the parameter range (14), equation (13) can be interpreted as follows: the gauge fluctuations couple the spinon-antispinon pair into an overdamped magnon resonance with mass gap

$$m_\Omega = 2m_s, \quad (15)$$

inverse life-time

$$\tau_\Omega^{-1} = \frac{T}{\chi m_s^2} g(0) Q_0 \lambda, \quad (16)$$

and T -dependent wave-function renormalization factor $Z_\Omega \sim \frac{\chi m_s Q_0}{T}$. In this respect, the situation is similar qualitatively to that appearing in the PG phase, but with different T and δ dependence of the parameters. Notice that typically in the SM phase $m_\Omega \ll \tau_\Omega^{-1}$, whereas in the PG phase $(m_\Omega)_{PG} \gg (\tau_\Omega^{-1})_{PG}$; that is to say, AF effect is more visible in the PG phase than in the SM phase.

The Green's function G for the 2D electron is given in real space by the product of the holon and the spinon propagators, averaged over gauge fluctuations. We are interested here in the quasi-particle pole, in particular in the temperature and doping dependence of the wave function renormalization constant Z and the damping rate Γ defined via a representation of the retarded electron correlation functions for small ω and momentum \vec{k}_F on the FS as

$$G^R(\omega, \vec{k}_F) \sim \frac{Z}{\omega + i\Gamma}. \quad (17)$$

To compute it we apply the dimensional reduction to the holon propagator by means of the tomographic decomposition introduced by Luther-Haldane.³¹ Following the procedure described in Ref. 14 we find within the range (14):

$$Z \approx \lambda_1 \left(\frac{Q_0}{k_F} \right)^{\frac{1}{2}} \left(\frac{m_s \kappa}{J^2} \right)^{\frac{1}{2}}. \quad (18)$$

Comparing it with the result in Ref. 14 one finds that the anisotropic weight present in the PG phase has disappeared. As this corresponds to a restoration of the full FS, this suggests again that the above results apply only away from the boundary of the PG/SM crossover in a parameter region where ALL effects due to PG have disappeared. The electron damping rate Γ at the FS is:

$$\Gamma = \frac{T}{2\chi m_s^2} Q_0 g(0) \lambda \propto T^{4/3} \frac{(1-\delta)^{5/3}}{\delta |\ln \delta|}. \quad (19)$$

We see that Γ is inversely proportional to the doping concentration.

IV. COMPARISON WITH EXPERIMENTS

A. In-plane Resistivity

The in-plane resistivity is one of the most studied properties of the High T_c cuprates. There is a narrow range of dopings characterizing optimal/slightly overdoped samples where the in-plane resistivity appear linear in T from T_c up to several hundreds Kelvin. In underdoped samples, it deviates from the linear dependence at low temperatures, first acquiring a sublinear behavior and then crossing an inflection point (which we take as the definition of the PG temperature T^*) and possibly (for strongly underdoped samples) reaching a minimum corresponding to the MIC whose origin was discussed at length in Ref 14. In overdoped samples above a critical doping concentration, one observes again deviation from linearity at low T , but there the behavior at low temperature is superlinear, eventually at high doping reaching a FL behavior $\sim T^2$. With increasing doping, one finds the temperature of deviation from linearity lowering in the underdoped region and increasing in the overdoped region. This has been taken as one of the experimental facts in favor of the existence of a QCP at $\delta \sim 0.19$ in Ref. 10.

To calculate the in-plane resistivity we apply the Ioffe-Larkin rule,³³

$$\rho = \rho_s + \rho_h. \quad (20)$$

Using the Kubo formula to calculate the spinon contribution to conductivity, within the range (14) one finds

$$\rho_s \simeq 2\lambda Q_0^{-1} (\Gamma + m_s^2/\Gamma) = \frac{T}{\chi m_s^2} g(0) \lambda^2 + \frac{4m_s^4 \chi}{T g(0) Q_0^2}. \quad (21)$$

In the high temperature limit $Q_0 \gg m_s$, the damping rate in (21) dominates over the spin gap $2m_s$ and the spinon contribution to resistivity is linear in T , with a slope $\alpha = g(0)\lambda^2/(\chi m_s^2) \simeq (1 - \delta)/(\delta |\ln \delta|)$. A linear in T behavior is also obtained in the gauge field theory of Nagaosa and Lee¹⁸ for the uniform RVB state with a very similar slope $\alpha_{RVB} \simeq 1/\delta$. Lowering the temperature, the second term in (21) gives rise first to a superlinear behavior and then, at the margin of validity (14) of our approach, an unphysical upturn. The deviation from linearity is due to the spin gap effects and is cutoff in the underdoped samples by the crossover to the PG phase. We expect that physically in the overdoped samples it is cutoff by a crossover to a FL “phase”.

We now turn to holon contributions. It is known since Nagaosa and Lee,¹⁸ that for a 2D Fermi gas scattering against a U(1) gauge field with Reizer-like singularity, the scattering time at the FS is proportional to $T^{-4/3}$. This power law follows simply from the scaling analysis and does not depend on the detail of the dispersion relations. The contribution ρ_h from our gas of spinless holons is of the form

$$\rho_h \sim \left(\frac{1}{\tau_{imp}} + \epsilon_F \left(\frac{T}{\epsilon_F} \right)^{4/3} \right), \quad (22)$$

where we also added the contribution of the impurity scattering via the Matthiessen rule. Compared with (21), it gives a subleading contribution. This could explain, as for the PG phase, the insensitivity of the resistivity to the presence of non-magnetic impurities which affect only ρ_h . The above results reproduce qualitatively the T –linearity of the in-plane resistivity in the SM phase, *including the decrease of the slope upon doping increase* and the superlinear behavior at low T for overdoped samples. One can use the deviation from linearity appearing in the overdoped samples to fix the phenomenological parameter λ at some doping by computing the scale independent quantity $(\rho(T) - \rho_h(0))/\alpha$ and comparing it with experimental data. The result is self-consistently determined as λ of the order 1, and more precisely, using LSCO data (for $\delta = 0.30$ ³⁴) one finds $\lambda \approx 0.7$ as quoted above. The temperature dependence of the spinon mass yields a bending at high temperature, stronger for lower dopings, as visible in the resistivity data at constant volume for LSCO;³⁴ this effect is masked in the resistivity data at constant pressure by thermal expansion.

In Fig. 1 we plot the in-plane resistivity given Eq.(21) versus temperature for different dopings. Except for an overall scale, once λ is fixed, there are no additional free parameters for other doping concentrations in Eq.(21) and the agreement with experiments is reasonably good.

We should mention that the linear temperature dependence of the in-plane resistivity is also reproduced in a number of theoretical studies, including the “marginal FL” theory,³⁵ the “hot spots”,^{9,21} as well as “cold spots”²² approaches, although the mechanism leading to the linear dependence varies from case to case, and is also somewhat different from ours.

B. Spin-Lattice Relaxation Rate

From the experimental point of view, one of the hallmarks of the SM phase is the unusually simple law for the spin-lattice relaxation rate at the Cu-sites:

$$\left(\frac{1}{T_1 T} \right)^{63} \sim \lim_{\omega \rightarrow 0} \sum_{\vec{q}} \frac{\text{Im} \chi_s(\omega, \vec{q})}{\omega} F(\vec{q}) \sim \frac{1}{T}. \quad (23)$$

where F is the hyperfine formfactor peaked around the AF wave vector \mathcal{Q}_{AF} . While in optimally doped samples the above proportionality relation is valid over a wide range of temperatures above T_c , in overdoped samples $(\frac{1}{T_1 T})^{63}$ saturates to a constant (i.e. T –independent) value at low temperatures, suggesting a possible crossover to a FL phase. Using the expression (10) for the magnon correlator one obtains a factorized form for the spin susceptibility: $\chi_s(\omega, \vec{q}) \sim \chi(\omega, \vec{q} = 0) \Xi(\vec{q})$ with $\int d^2 \vec{q} \Xi(\vec{q}) = 1$, a feature present also in the PG phase and that has been claimed to be in agreement with experimental data.³⁶

Then in our computation we are left with the following integral:

$$\left(\frac{1}{T_1 T} \right)^{63} \sim (1 - \delta)^2 \int dx^0 i x^0 \frac{1}{x^{02}} e^{-2im_s x^0 - \frac{T}{2\chi m_s^2} g(0) Q_0^2 x^{02}}. \quad (24)$$

Up to the factor $(1 - \delta)^2$, the above integral is equal to the spinon contribution to the conductivity.

Therefore, in the high temperature limit we recover the linear in T behavior for $(T_1 T)^{63} \approx T/((1 - \delta)^2 \chi m_s^2)$ and at high doping and low temperature the superlinear deviation, also found experimentally in overdoped samples of LSCO.³⁷ Furthermore, the factor $(1 - \delta)^{-2}$ weakens the doping dependence of the slope as compared with the resistivity curves, in agreement with the experimental data. In Fig. 2 we plot $1/T_1^{63}$ extracted from Eq.(24) versus temperature for different dopings.

C. Out-of-plane Resistivity

Conductivity along the c -axis in cuprates appears as mainly due to the interlayer tunneling process. Since there is no measurable Fermi velocity along this axis because of very small (effective³⁸) hopping integral t_c , we can use Kumar-Jayannavar (K-J) approach to calculate $\rho_c(T)$. According to these authors,³⁹ the out-of-plane motion in cuprates is incoherent and governed by the strong in-plane scattering via the quantum blocking effect. At high temperatures $\Gamma \gg t_c$ the interlayer tunnelling rate is reduced by the in-plane scattering. Under these assumptions, $\rho_c(T)$ is controlled by the second term in the K-J formula:

$$\rho_c \sim \frac{1}{\nu} \left(\frac{1}{\Gamma} + \frac{\Gamma}{t_c^2 Z^2} \right). \quad (25)$$

In the SM phase, substituting Γ and Z with the corresponding estimates (19) and (18) in (25), we recover the T -linearity in the “incoherent regime” $\Gamma \gg t_c Z$:

$$\rho_c \simeq \frac{J^2}{t_c^2} \frac{k_F}{m_s \nu(\epsilon_F) \kappa} \frac{T}{2\chi m_s^2} \simeq \frac{T}{(\delta |\ln \delta|)^{3/2}} \quad (26)$$

decreasing faster than $\rho_{ab}(T)/T$ upon doping increase.

The out-of-plane resistivity was also calculated in a number of theoretical studies, including the gauge field approach⁴⁰ and “cold spots” model.²² As far as we understand, the correct temperature dependence in the SM phase could not be reproduced there.

Equation (25) would predict a minimum in ρ_c at low T , unless it is cutoff by a crossover to a new “phase”. Hence, in the spin-charge gauge approach ρ_c might exhibit a MIC for three different reasons, each one with its own T and δ dependence: 1) a K-J minimum in the PG phase 2) a minimum due to a crossover from an insulating regime in the PG phase to a metallic regime in the SM phase 3) a K-J minimum in the SM phase. Most of the MIC in ρ_c exhibited in the experimental data appear to correspond to the second case; thus the minimum roughly corresponds to the deviation from linearity. The first case is usually cutoff by the crossover to the SM. Perhaps an example of the third case is the minimum found in BSCCO at $\delta \approx 0.225$ ⁴¹ suppressing superconductivity with a magnetic field, as the minimum there is lower than the deviation from linearity. However, the parameter region where this minimum has been found is close to the boundary of the SM phase, so one could expect corrections to our formulas that has to be investigated. In Fig. 3 we plot ρ_c extracted from Eq.(25) versus temperature for different doping concentrations and a fixed value of the relative coefficient of the metallic versus insulating term, $r \sim J^2/(t_c^2 \lambda_1^2)$ (with λ_1 as given in Eq.(18)) and compare the result with data in LSCO.⁴²

Unfortunately, we don’t have a reliable method to estimate the (extrapolated) $T = 0$ intercept of $\rho_c(T)$ which is large when compared with the corresponding intercept for ab -plane resistivity, and it is also difficult to fix precisely using experimental data the relative coefficient r , so we cannot extract safely the anisotropy ratio $\rho_c(T)/\rho_{ab}(T)$. However, let us notice that if the minimum in ρ_c is at higher temperature than the (unphysical) minimum in ρ_{ab} , then one can derive the fast decrease of the anisotropy ratio at low temperature found experimentally,⁴² see Fig.4.

Finally let us propose a simple qualitative explanation of the linear T -behavior of both in-plane and out-of-plane resistivity in the “interior” of the SM phase in terms of “effectiveness” in the momentum space, somewhat analogous to the “effectiveness” appearing, in the coordinate space, in the treatment of anomalous skin effect (see e.g. Ref. 43). In our approach the electron resonance life-time was found to be $\tau_e \sim T^{-\frac{4}{3}}$, so that from Boltzmann transport formula naively one expects to find a conductivity $\sigma_0 \sim T^{-\frac{4}{3}}$. However the gauge field is able to combine spinon and holon into a resonance only in a range of momenta of the order of the anomalous skin momentum $Q_0 \sim T^{\frac{1}{3}}$, so only a fraction of electrons Q_0/p_F should contribute or be “effective” for conductivity, so that $\sigma \sim \sigma_0 Q_0 \sim T^{-\frac{4}{3}} T^{\frac{1}{3}} = T^{-1}$.

D. AC conductivity

A key feature of AC conductivity in the SM phase is a tail $\sim \omega^{-1}$, found already in earlier experiments. However recently it has been observed (in LSCO⁴⁴ and BSCO⁴⁵) that it is related to an asymmetric peak structure in overdoped samples centered at a finite frequency, increasing with doping, shifting to higher frequency and symmetrizing when the temperature increases beyond the peak frequency at low T . All these features are qualitatively reproduced in our spin-charge gauge approach. As explained in Ref. 15, to compute the AC conductivity one first evaluates the thermal gauge propagator with UV cutoff in the ω -integration given by $\Lambda = \max(T, \Omega)$, where Ω is the external frequency and as usual the thermal function $\coth \omega/T$ is approximated by T/ω and $\text{sign} \omega$ in the two limits $\Omega \ll T, T \ll \Omega$, respectively. It turns out that up to the logarithmic accuracy one can pass from the first to the second limit by

replacing T with Ω in Q_0 and Γ (we denote the obtained quantities by Q_Ω, Γ_Ω) and rescaling the f and g functions resulting from the gauge field integration, by a positive multiplicative factor $\tilde{\lambda} \lesssim 1/2$. It is straightforward then to derive the leading spinon contribution to the AC conductivity at finite T in the two limits. For $\Omega \ll T$ we have

$$\sigma(\Omega, T) \sim \frac{Q_0}{i(\Omega - 2m_s) + \Gamma} \sim \frac{1}{i(\Omega - 2m_s)T^{-1/3} + T}, \quad (27)$$

while for $T \ll \Omega$

$$\sigma(\Omega, T) \sim \frac{Q_\Omega}{i(\Omega - 2m_s) + \tilde{\lambda}\Gamma_\Omega} \sim \frac{1}{i(\Omega - 2m_s)\Omega^{-1/3} + \Omega}. \quad (28)$$

From the above formulas the features discussed at the beginning of this subsection are easily derived: the tail $\sim \Omega^{-1}$ is evident and the effect of replacing Q_0 by Q_Ω is to asymmetrize the peak at $2m_s$ appearing in $\text{Re}\sigma(\Omega, T)$ for $\Omega \ll T$ and to shift it towards lower frequency. The optical conductivity was discussed in a number of theoretical studies, including the spin-fermion approach,⁹ “nearly AF Fermi liquid” theory²¹ and “cold spots” model.²² To the best of our knowledge, the above considered features were not addressed earlier. In Fig. 5 we plot the AC conductivity in the two regimes considered above at fixed doping. Inclusion of the contribution of holons via Ioffe-Larkin rule does not change the qualitative features, but enhances the finite temperature curves, improving the agreement with experiments.

Two remarks are in order. First, our formulas do not apply for Λ close to zero, where we expect a transition to a different “phase” as discussed above. Second, one can prove that the peak seen in the SM phase is replaced in the PG phase by a broad maximum (moving to lower frequency as doping increases), due to the “relativistic” structure of the spinon peculiar to that phase, as discussed in Ref. 15.

V. CONCLUDING REMARKS

To conclude we have shown that the spin-charge gauge approach originally proposed to describe the PG phase of the cuprate superconductors, in particular, the MIC in the underdoped cuprates can be generalized to the SM phase as well. The common features are the interplay of the AFSRO and the gauge field fluctuations, which leads to magnon and electron resonances, while the difference is the presence of a statistical π -flux lattice for holons in the PG phase responsible for the small “Fermi-arcs” and its absence in the SM phase. As the doping/temperature increases the MIC is taking place, and then the flux lattice “melts”. It is interesting to observe that the extrapolations from the PG and SM regions more or less match each other in the crossover area. In some sense the PG treatment is doing a “better job”, producing the MIC and sublinear temperature dependence for the in-plane resistivity, up to the inflection point T^* as the margin of the PG phase. It is true that the “high temperature asymptotics” $\sim T^{1/4}$ derived in the PG phase does not correspond to experiment, but that has been corrected by the SM consideration and the disappearance of the “Fermi-arcs” feature allows to recover the celebrated linear in T dependence. This dependence in our approach can be interpreted as due to the combined effect of an electron life time $\sim T^{-\frac{4}{3}}$ due to gauge interactions triggered by Reizer singularity, and the “effective” slab in momentum space where the electron resonance forms $\sim Q_0 \sim T^{\frac{1}{3}}$, with Q_0 as the anomalous skin momenta again associated with the Reizer singularity.

In our view there seems to be a crossover line between the ‘insulating’ and ‘metallic’ regions at any finite temperature. Probably, this crossover becomes a quantum phase transition at zero temperature between the AFSRO state and FL state, although the transition point seems not being able to control the behavior of the system over a large region, because of the appearance of new scales (AF correlation length) nearby. This scenario seems in consistency with the picture extracted from the μ SR measurements in the SC state.⁴⁶ The phase diagram that our approach suggests is in a sense intermediate between the RVB and the QCP picture, sharing with the first scenario the nature of crossover for the border between the PG and SM phases at finite T , while with the second scenario the existence of a true phase transition at $T = 0$.

APPENDIX

In this Appendix, using Ref. 11 as a guideline, we show how to satisfy on average the *Assumption 0*. We split the integration over V into an integration over a field $V^{(c)}$, satisfying the Coulomb condition:

$$\partial^\mu V_\mu^{(c)} = 0, \quad (\text{A.1})$$

and its gauge transformations expressed in terms of an $SU(2)$ -valued scalar field g , i.e., $V_a = g^\dagger V_a^{(c)} g + g^\dagger \partial_a g$, $a = 0, 1, 2$.

Integrating over the time component of the C-S gauge fields one finds:

$$B_\mu = \bar{B}_\mu + \delta B_\mu, \quad \delta B_\mu(x) = \frac{1}{2} \sum_j H_j^* H_j \partial_\mu \arg(x - j), \quad (\text{A.2})$$

where \bar{B}_μ gives rise to a π -flux phase, i.e., $e^{i \int_{\partial p} \bar{B}} = -1$ for every plaquette p and

$$V_\mu^{(c)} = \sum_j (1 - H_j^* H_j) (\sigma_x^{[j]} g_j^\dagger \frac{\sigma_a}{2} g_j \sigma_x^{[j]})_{11} \partial_\mu \arg(x - j) \sigma_a, \quad (\text{A.3})$$

where σ_a , $a = x, y, z$ are the Pauli matrices. It is not difficult to see that the statistical field $V^{(c)}$ defined in (A.3) does not carry flux π per plaquette, so that strictly speaking the constraint $\arg(U_{\partial p}) = 0$ cannot be satisfied. However, it is sufficient for our purposes that whenever a hole make a closed loop on the lattice, it acquires a trivial phase factor ($2\pi n$).

At the lattice level, the particle can either stay at rest at a given site or jump to a nearest neighbor.

Without loss of generality, we consider a holon going around a given plaquette p counterclockwise.

Now assume that the particle hops from site i to site j . Let $\underline{\omega}$ denote the set of trajectories of holons in a first-quantization path representation. In such formalism the trajectories are left continuous in time, i.e. one should think of the holon in the link located at the end of the jump. It is shown in Ref 11 that for the optimal configuration, independently of δ ,

$$\left(\sigma_x^{[i]} g_i^\dagger e^{i \int_{<i,j>} V^{(c)}} g_j \sigma_x^{[j]} \right)_{11} \simeq \left(\sigma_x^{[i]} \tilde{g}_i^\dagger \tilde{g}_j \sigma_x^{[j]} \right)_{11}. \quad (\text{A.4})$$

where the $SU(2)$ variables \tilde{g}_i, \tilde{g}_j have the structure:

$$\tilde{g}_i = e^{i \theta_i \sigma_z}, \quad i \notin \underline{\omega} \quad (\text{A.5})$$

$$\tilde{g}_j = i(\vec{\sigma} \cdot \vec{n}_j), \quad n_j = (\cos \phi_j, \sin \phi_j, 0), \quad j \in \underline{\omega} \quad (\text{A.6})$$

with θ_j and ϕ_j so far arbitrary angles.

These degrees of freedom will be fixed in order to cancel the π -magnetic flux per plaquette generated by \bar{B} . We need to impose:

$$\prod_{<i,j> \in \partial p} \left(\sigma_x^{[i]} \tilde{g}_i^\dagger \tilde{g}_j \sigma_x^{[j]} \right)_{11} = e^{i\pi}. \quad (\text{A.7})$$

Writing out explicitly the left-hand side of (A.7), we find

$$e^{i(\theta_1 + \phi_2)} e^{-i(\theta_2 + \phi_4)} e^{i(\theta_4 + \phi_3)} e^{-i(\theta_4 + \phi_1)} \quad (\text{A.8})$$

which is satisfied by the choice $\phi_j = \frac{\pi}{4}(-1)^{|j|}$ irrespective of the θ_j phases, provided the latter contributes with a trivial phase factor.

Using this gauge freedom we can be even more demanding, by requiring that the field \bar{B} is exactly cancelled link by link. For instance, imposing

$$\theta_j = -\frac{\pi}{2}(-1)^{|j|},$$

we cancel the distribution of phase factors for \bar{B} chosen in Ref 11. This proves that choosing the $SU(2)$ gauge field as described above, the *Assumption 0* is satisfied.

Acknowledgments. One of us (P.M.) wishes to thank C. Pepin, G. Qin and T. Zillio for useful discussions and the Chinese Academy of Sciences for kind hospitality. Interesting discussions with T. Xiang are gratefully acknowledged.

¹ See, *e.g.*, the recent review M.R. Norman and C. Pépin, Rep. Progr. Phys. **66**, 1547(2003).

- ² G. Baskaran, Z. Zou, and P.W. Anderson, Solid State Commun. **63**, 973 (1987); G. Kotliar and J. Liu, Phys. Rev. B **38**, 5142 (1988); H. Fukuyama, Progr. Theor. Phys. Suppl. **108**, 287 (1992); N. Nagaosa and P.A. Lee, Phys. Rev. B **45**, 966 (1992).
- ³ See, *e.g.*, S. Sachdev, “Quantum Phase Transitions”, Cambridge University Press, 1999.
- ⁴ S. Sachdev, Rev. Mod. Phys. **75**, 913 (2003).
- ⁵ S.A. Kivelson *et al.*, Rev. Mod. Phys. **75**, 1201 (2003).
- ⁶ C. M. Varma Phys. Rev. B **55**, 14554 (1997); S. Chakravarty, R.B. Laughlin, D. Morr, and C. Nayak Phys. Rev. B **63**, 094503 (2001).
- ⁷ C. Castellani *et al.*, Z. Phys. B **103**, 137 (1997); J. Phys. Chem. Solids **59**, 1694 (1998).
- ⁸ D. Pines, Z. Phys. B **103**, 120 (1997) and references therein.
- ⁹ Ar. Abanov, A.V. Chubukov, and J. Schmalian, Adv. Phys. **52**, 119 (2003) (See cond-mat/0107421).
- ¹⁰ J.L. Tallon *et al.*, Phys. Stat. Sol. (b) **215**, 531 (1999); J.L. Tallon *et al.*, cond-mat/0211048.
- ¹¹ P.A. Marchetti, Z.B. Su, L. Yu, Phys. Rev. B **58**, 5808 (1998).
- ¹² P.A. Marchetti, J.H. Dai, Z.B. Su and L.Yu, J. Phys. Condens. Matt. **12**, L329 (2000).
- ¹³ P.A. Marchetti, Z.B. Su and L. Yu, Phys. Rev. Lett. **86**, 3831 (2001).
- ¹⁴ P.A. Marchetti, L. De Leo, G. Orso, Z.B. Su and Yu Lu, Phys. Rev. B **69** 024527 (2004).
- ¹⁵ P.A. Marchetti, G. Orso, Z.B. Su and Yu Lu, to appear in Phys. Rev. B (LH9601BJ).
- ¹⁶ A. Damascelli, Z. Hussain, and Z.X. Shen, Rev. Mod. Phys. **75**, 473 (2003).
- ¹⁷ See, *e.g.*, H. Fukuyama, Progr. Theor. Phys. Suppl. **108**, 287 (1992).
- ¹⁸ P.A. Lee and N. Nagaosa, Phys. Rev. Lett. **65**, 2450 (1990); Phys. Rev. B **46**, 5621(1992).
- ¹⁹ L.B. Ioffe and P.B. Wiegmann, Phys. Rev. Lett. **65**, 653 (1990); L.B. Ioffe and G. Kotliar, Phys. Rev. B **42**, 10345 (1990).
- ²⁰ I. Ichinose *et al.*, Phys. Rev. B **64**, 104516 (2001).
- ²¹ B.P. Stojkovic and D. Pines, Phys. Rev. B **55**, 8576, **56**, 11931 (1997).
- ²² L.B. Ioffe and A.J. Millis, Phys. Rev. B **58**, 11631 (1998); see, also, A.T. Zheleznyak *et al.*, Phys. Rev. B **57**, 3089 (1998).
- ²³ J. Fröhlich and P.A. Marchetti, Phys. Rev. B **46**, 6535 (1992).
- ²⁴ R. T. Birgeneau *et al.*, Phys. Rev. B **38**, 6614 (1988).
- ²⁵ M. Reizer, Phys. Rev. B **39**, 1602 (1989); **40**, 11571 (1989).
- ²⁶ E.H. Lieb, Phys. Rev. Lett. **73**, 2158 (1994).
- ²⁷ J. Bellisard and R. Rammal, Europhys. Lett. **13**, 205 (1990).
- ²⁸ G. Qin, unpublished.
- ²⁹ B. Keimer *et al.*, Phys. Rev. B **46**, 14034 (1992).
- ³⁰ G. Orso, Ph. D. Thesis, SISSA, 2003.
- ³¹ A. Luther, Phys. Rev. B **19**, 320 (1979); F.D.M. Haldane, Varenna Lectures 1992.
- ³² G. Benfatto, G. Gallavotti, J. Stat. Phys. **59**, 541 (1990); R. Shankar, Rev. Mod. Phys. **66**, 129 (1994).
- ³³ L. Ioffe and A. Larkin, Phys. Rev. B **39**, 8988 (1989).
- ³⁴ B. Sundqvist and E.M.C. Nilsson, Phys. Rev. B **51**, 6111 (1995); K. Takenaka *et al.*, Phys. Rev. B **68**, 134501 (2003).
- ³⁵ C.M. Varma *et al.*, Phys. Rev. Lett. **63**, 1996 (1989).
- ³⁶ P.B. Littlewood, in “Strongly interacting fermions and High T_c superconductivity”, Proceedings, Les Houches 1991.
- ³⁷ C. Berthier *et al.*, J. Physique I **6**, 2205 (1997); S. Fujiyama *et al.*, J. Phys. Soc. Jpn. **66**, 2864 (1997).
- ³⁸ For simplicity we neglect the k -dependence of the hopping integral, replacing it by an averaged effective constant hopping parameter t_c .
- ³⁹ N. Kumar and A.M. Jayannavar, Phys. Rev. B **45**, 5001 (1992); N. Kumar *et al.*, Mod. Phys. Lett. B **11**, 347 (1997); Phys. Rev. B **57**, 13399 (1998).
- ⁴⁰ N. Nagaosa, Phys. Rev. B **52**, 10561 (1995).
- ⁴¹ L. Krusin Elbaum *et al.*, Int. J. Mod. Phys. B **17**, 3598 (2003).
- ⁴² Y. Nakamura and S. Uchida, Phys. Rev. B **47**, 8369 (1993).
- ⁴³ J Callaway, “Quantum Theory of the Solid State”, Academic Press, 1991
- ⁴⁴ T. Startseva *et al.*, Physica C **321**, 135 (1999).
- ⁴⁵ S. Lupi *et al.*, Phys. Rev. B **62**, 12418 (2000).
- ⁴⁶ C. Panagopoulos *et al.*, Solid State Commun. **126**, 47 (2003)

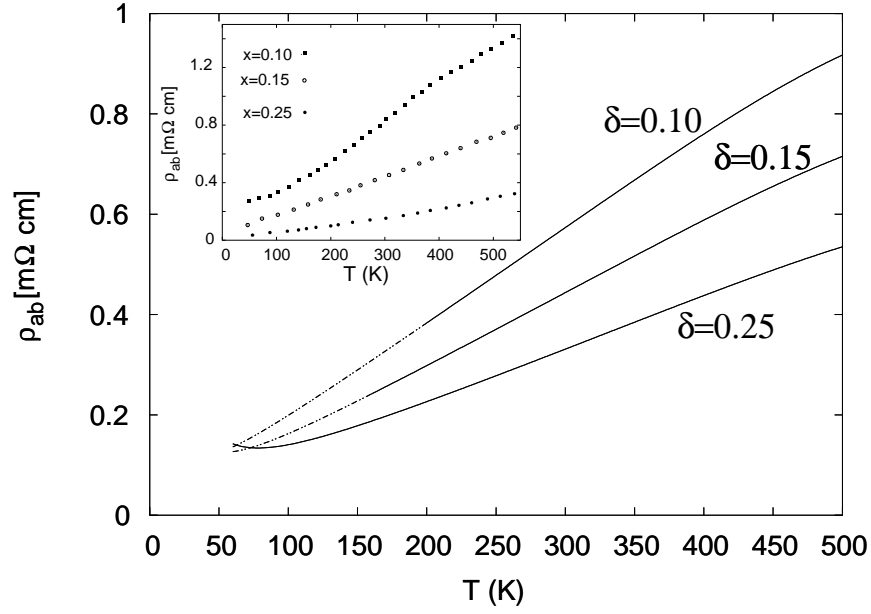


FIG. 1: Calculated in-plane resistivity as a function of temperature for different hole concentrations. Below the pseudo-gap temperature T^* , the curve is shown in dashed line. The resistivity scale is fixed by comparison with experimental data for $\delta = 0.15$ at 400 K. *Inset*: In-plane resistivity versus T measured in LSCO crystals with different Sr content x , taken from the work of Takenaka *et al.*, Ref. 34

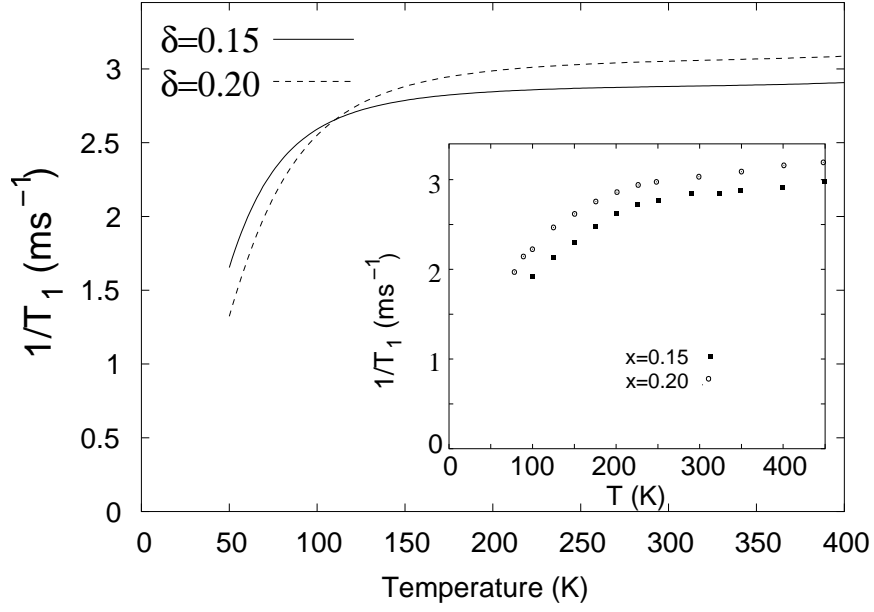


FIG. 2: Calculated temperature dependence of the spin-lattice relaxation rate $1/T_1$ for different doping concentrations. *Inset*: spin-lattice relaxation rate measured in LSCO samples with different Sr content x , taken from the work of Fujiyama *et al.*, Ref. 37.

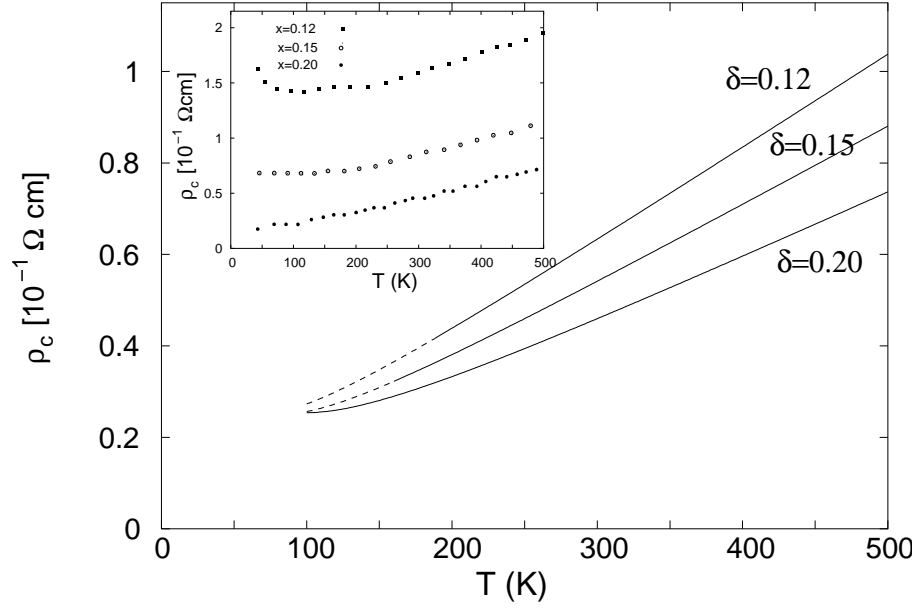


FIG. 3: Calculated out-of-plane resistivity as a function of temperature for different hole concentrations. Below the pseudo-gap temperature T^* , the curve is shown in dashed line. *Inset*: In-plane resistivity versus T measured in LSCO crystals with different Sr content x , taken from the work of Nakamura *et al.*, Ref. 42

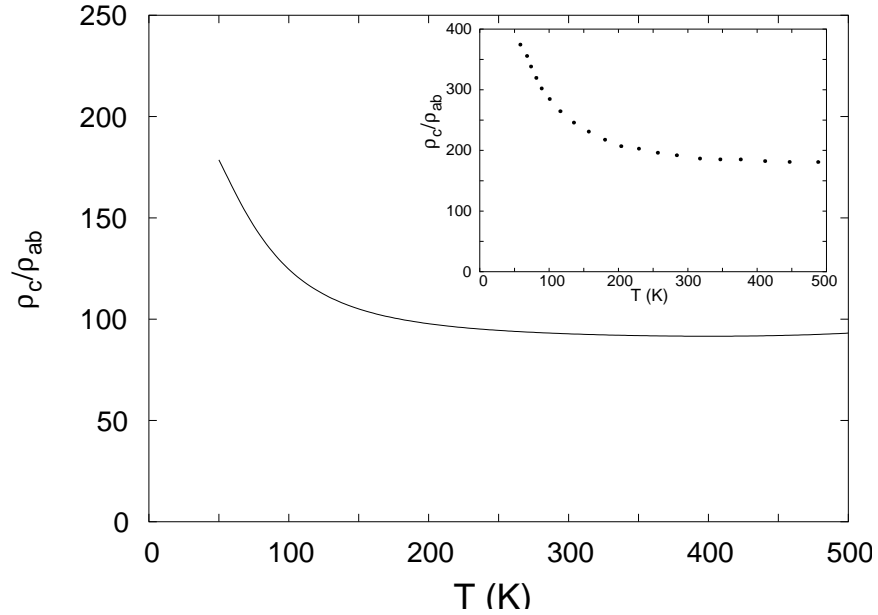


FIG. 4: Calculated resistivity anisotropy ratio as a function of temperature for fixed hole density $\delta = 0.2$. *Inset*: resistivity anisotropy ratio measured for a LSCO sample with Sr content $x = 0.20$, taken from the work of Nakamura *et al.*, Ref. 42.

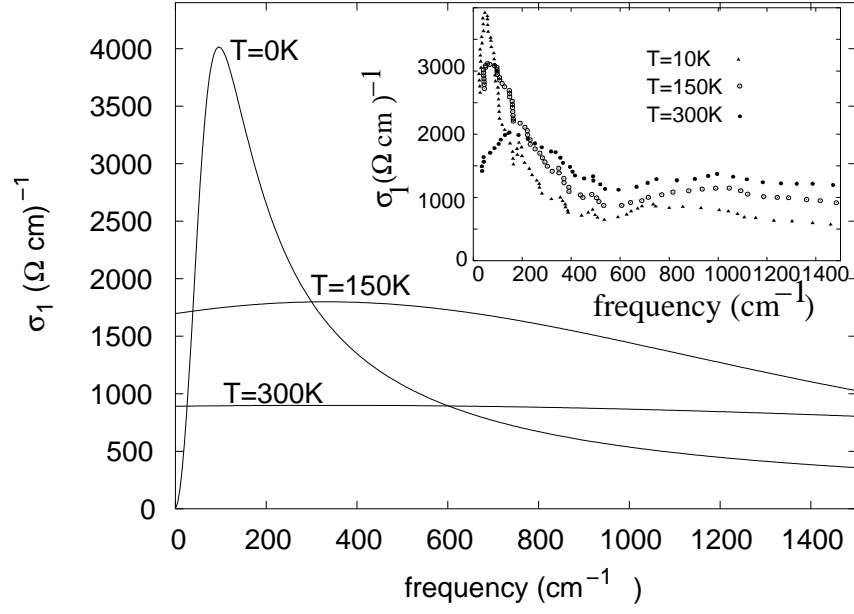


FIG. 5: Calculated AC conductivity as a function of frequency for fixed hole density $\delta = 0.184$ and different temperatures. *Inset*: AC conductivity versus frequency measured for a LSCO sample with $x = 0.184$ at different temperatures, taken from the work of Startseva *et al.*, Ref. 44.